SCIENCE CHINA
Chemistry

•MINI REVIEWS•
SPECIAL ISSUE: 2024 Emerging Investigator Issue

https://doi.org/10.1007/s11426-024-2344-0

Mechanochemistry of cyclobutanes

Roberto Obregon & Junpeng Wang*

School of Polymer Science and Polymer Engineering, University of Akron, Akron, OH 44325, USA

Received September 12, 2024; accepted September 30, 2024; published online November 11, 2024

The field of polymer mechanochemistry has been revolutionized by implementing force-responsive functional groups—mechanophores. The rational design of mechanophores enables the controlled use of force to achieve constructive molecular reactivity and material responses. While a variety of mechanophores have been developed, this Mini Review focuses on cyclobutane, which has brought valuable insights into molecular reactivity and dynamics as well as innovations in materials. We discuss its reactivity and mechanism, dynamics and stereoselectivity, as well as impacts on material properties.

mechanochemistry, mechanophore, cyclobutane

Citation: Obregon R, Wang J. Mechanochemistry of cyclobutanes. *Sci China Chem*, 2024, 67, https://doi.org/10.1007/s11426-024-2344-0

1 Introduction

When it comes to triggering a reaction, chemists often think of heat or light. A less common yet intriguing way to initiate reactions is through mechanical force. What makes using force as a stimulus unique is it is directional, which allows for engineering reactivity with both the magnitude and direction of force [1]. Over the past two decades, the field of polymer mechanochemistry has experienced rapid growth, largely fueled by the concept of force-responsive moiety—the mechanophore [2], which enables controlled reactivity and constructive responses in materials. Self-strengthening [3], stress sensing [4], and controlled drug release [5,6] are among some of the applications of mechanophores.

Mechanophores can generally be categorized into scissile mechanophores and nonscissile mechanophores (Figure 1) [7]. In a typical case, the mechanophore is on the polymer backbone, and the activation of the mechanophore causes different outcomes for the polymer chain for a scissile mechanophore *vs*. a nonscissile mechanophore: activation of the former breaks the polymer chain into two parts while activation of the latter does not lead to the breakage of the polymer chain.

While there are different mechanophores in use, this Mini Review will focus on cyclobutane, which, in response to mechanical force, can undergo cycloreversion to form two alkenes (Figure 2a). Compared to most other mechanophores developed to date, cyclobutane has several unique features. First, the cycloreversion of an unsubstituted cyclobutane requires an activation energy of 58–60 kcal/mol [8], which renders it thermally stable. For example, a thermal decomposition study of cyclobutane by Walters and co-workers [9] showed that cyclobutane has a half-life of 3 h at 420°C. Second, mechanically generated alkenes are useful for building conjugated structures [10] and for downstream reactions, such as thiol-ene reaction [11] and olefin metathesis [12]. Third, cyclobutane can be conveniently incorporated through photochemical [2+2] cycloaddition reactions [13] or polyaddition of cyclobutene [14].

In 2010, Moore and co-workers [15] reported the generation of cyanoacrylates from the mechanical cleavage of a dicyanocyclobutane (Figure 2b), which represents the first example of mechanochemical activation of cyclobutane. Note that cyclobutane is a scissile mechanophore. In 2012, Craig and co-workers [16] demonstrated that a nonscissile mechanophore can be made by fusing cyclobutane with an-

*Corresponding author (email: jwang6@uakron.edu)

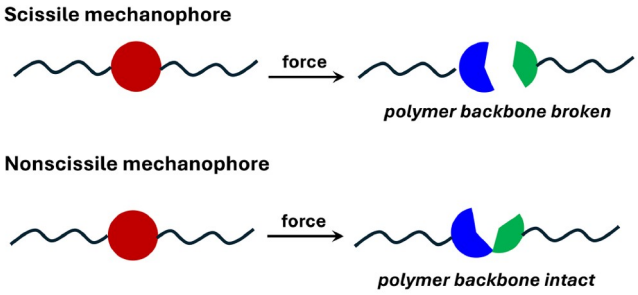

Figure 1 (Color online) Distinction between a scission mechanophore and a nonscissile mechanophore.

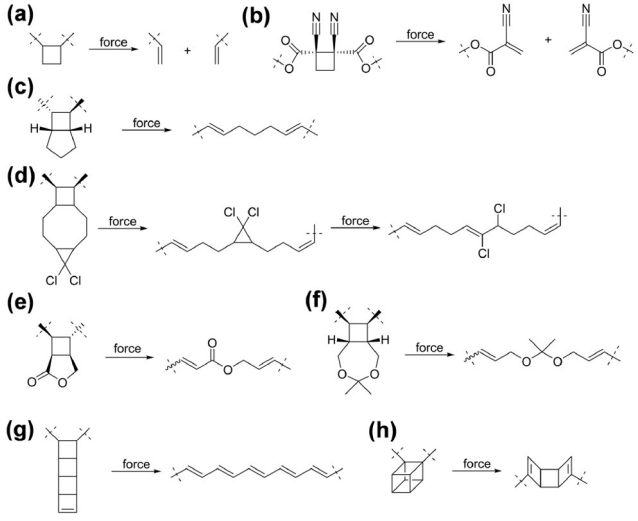

Figure 2 (a–h) Representative examples of cyclobutane-based mechanophores and their corresponding mechanochemical transformations.

other ring (Figure 2c). Nonscissile mechanophore enables the constructive transformation of multi-mechanophore polymers, which facilitates the characterization of the mechanochemical reactions. In 2013, Craig and co-workers [11] synthesized a series of polymers that contain cyclobutane-fused cyclohexane (CBCH) in their repeat units. The CBCH polymers allowed them to systematically investigate the reactivity and mechanism of the mechanochemical cycloreversion, which will be discussed in detail in the section of Reactivity and Mechanism. The activation of nonscissile cyclobutane-based mechanophores in multi-mechanophore polymers also facilitates the single-molecule force spectroscopy (SMFS) measurement of the force required to activate cyclobutane. In 2016, Craig and co-workers [17] reported that the force required to activate the cycloreversion of cyclobutane on a time scale of 100 ms to be 2.2 nN, according to SMFS characterization. Moreover, the nonscissile cyclobutane-based mechanophore also inspired the concept of mechanical gating. For example, when a second mechanophore is placed in the ring next to cyclobutane, it does not experience force until cyclobutane is activated first (Figure 2d). This mechanical gating concept was further developed by Wang (Figure 2e) and Craig's group (Figure 2f) [17] to control the degradation of polymers; when a degradable functional group is introduced into the ring that is fused to cyclobutane, the degradable group is not brought to the polymer backbone until the cyclobutane undergoes mechanochemical cycloreversion. Mechanically gated polymers have been discussed in length by other review articles on mechanochemical degradation of polymers [18,19] and will not be a focus of this review. Furthermore, Xia and co-workers [10] leveraged the nonscissile cyclobutane-based mechanophore and the generation of alkenes to make conjugated polymers by mechanochemical activation of polyladderene. Other notable and intriguing cyclobutane-based mechanophores include cubane [20], cinnamate dimer [21–23], and coumarin dimer [24–26]. In addition, Xia's group [27] and Moore's group [28] reported interesting dynamics of the mechanochemical cycloreversion of cyclobutane. Importantly, Craig's group [29–31] incorporated cyclobutane in polymer networks and achieved new material properties.

In addition to cyclobutane, the four-membered ring hydrocarbon, other four-membered rings containing heteroatoms were also explored as mechanophores, such as the β-lactam that undergoes mechanochemically induced retro-Staudinger cycloaddition to form ketene and imine, as reported by Moore's group [32], and the 1,2-azetidinone that can be mechanically activated to generate isocyanate and imine, as reported by Craig's group [33].

The development of the cyclobutane mechanochemistry noted above prompted us to write this Mini Review. In it, we aim to dive into the following three aspects, including reactivity and mechanism, dynamics and stereoselectivity, and advancements in material design. We will also discuss our perspective and outlook regarding the development and application of this mechanophore.

2 Reactivity and mechanism

We begin the discussion not on cyclobutane or mechanophores, but instead on what it means to have a mechanochemical reaction. There is an analogy if one considers traditional chemical reactions. A mechanically activated reaction is accelerated by lowering the activation energy with the mechanical work (Figure 3) exerted into the system:

$$\Delta E_0 - \Delta E_F = F\Delta x^{\dagger} \quad (1)$$

$\Delta x^{\dagger}$ termed activation length, is the distance the polymer backbone extends as the mechanophore is converted from the ground state to the transition state [34]. It quantitatively gauges how force efficiently couples to a certain system. Note that Eq. (1) assumes that the distance $\Delta x^{\dagger}$ from the reactant to the transition state does not change as a function

of force but that perturbations are possible [35–37]. Following from Eq. (1), the rate of a given mechanochemical reaction (i.e., the reactivity of a given mechanophore) is therefore given by

$$k(F) = k_0 \exp\left(\frac{F\Delta x^{\dagger}}{k_B T}\right) \quad (2)$$

In Eq. (2), $k(F)$ represents the rate constant when force F is applied, k_0 represents the force-free rate constant, k_B is the Boltzmann constant, and T is the temperature. Compared to thermal chemistry, mechanochemistry is distinct in that the mechanochemical reactivity can be tailored by altering both the force-free reactivity k_0 and the activation length $\Delta x^{\dagger}$. A structural variation could alter one or both factors.

The two main solution-based techniques that have been used to study the reactivity and mechanism of mechanochemical activation are ultrasonication and single-molecule force spectroscopy (SMFS) (Figure 4). Ultrasonication applies force to polymers through cavitation generated by the ultrasound waves. When the cavitation bubbles collapse, the chain around the bubble is rapidly elongated via solvodynamic shear and is subjected to force [38]. The advantages of ultrasonication include convenient operation and a suitable laboratory scale for spectroscopic characterization of the mechanochemical activation products. SMFS measurement

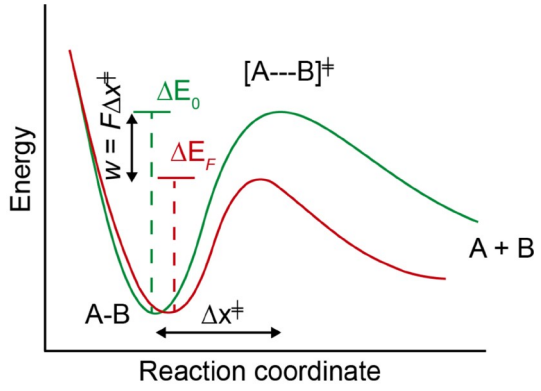

Figure 3 (Color online) Representation of the potential energy surface of a reaction in the absence of a coupled force (green) and in the presence of a coupled force (red).

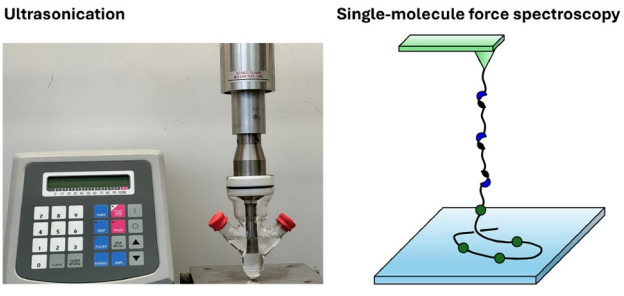

Figure 4 (Color online) Ultrasonication (left) and single-molecule force spectroscopy (right).

is conducted by forming a polymer bridge between the tip and substrate of an atomic force microscope (AFM) and measuring the restoring force and extension on the polymer as the AFM tip and substrate are separated [39]. SMFS is a powerful technique in characterizing mechanochemical reactivity, as it provides quantitative information on the force applied to mechanophores and the geometric changes of the mechanophores during mechanochemical transduction [21,34,40–43].

2.1 Mechanism and stereoselectivity

The mechanochemical cycloreversion of cyclobutane involves mechanically breaking the cyclobutane ring to form two alkenes. Mechanistic studies by Kean *et al.* [11] on a bicyclo[4.2.0]octane (BCO) showed that mechanochemical cycloreversion of cyclobutane most likely proceeds through a stepwise mechanism, and the breakage of the C1–C2 bond that generates the diradical intermediate is the rate-limiting step (Figure 5). After the breakage of the C1–C2 bond, the rotation along the C1–C4 bond and/or the C2–C3 bond before the cleavage of the C3–C4 bond leads to stereochemically distinct products, specifically *EE*, *EZ*, and *ZZ* alkenes. The observation of a mixture of *EE*, *EZ*, and *ZZ* alkenes from the mechanochemical activation of BCO and other cyclobutane-based mechanophores supports that the mechanochemical cycloreversion goes through a stepwise as opposed to a concerted mechanism.

2.2 Substituent effect

The putative diradical mechanism indicates that functional groups that can stabilize the diradicals will increase the reactivity and lower the force required to activate the mechanophore. Electronegativity, conjugation, and steric hindrance can contribute to the stabilization. For example, Kryger *et al.* [44] have shown that attaching a cyano group to cyclobutane can enhance the reactivity, and the reactivity can be further promoted by adding another cyano group (Figure 6a). The increased reactivity was attributed to steric effects from the cyano groups.

Note that the cyano group in the work by Kryger *et al.* [44] is not on the polymer backbone; in other words, force does not apply to the cyano group. When a substituent is also on the polymer backbone, e.g., the phenyl groups shown in Figure 6b, both the force-free reactivity k_0 and the activation length $\Delta x^{\dagger}$ can be affected. According to the SMFS study by Craig and co-workers [29], the phenyl substitution in Figure 6b can reduce the threshold force from 2 to 1 nN.

2.3 Stereochemical effect

Stereochemistry of the pulling attachment can significantly

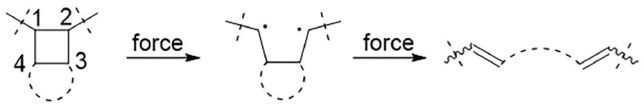

Figure 5 Putative mechanism for the mechanochemical cycloreversion of cyclobutane.

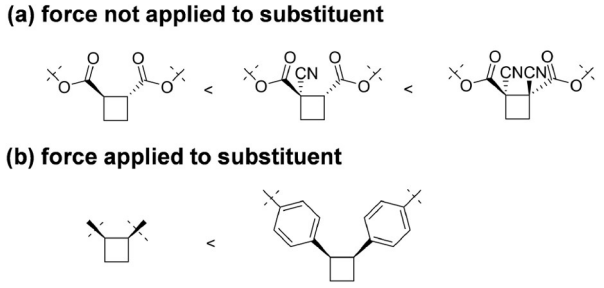

Figure 6 (a, b) Examples of two types of substituent effect. The structures are shown based on the order of reactivity.

impact the mechanochemical reactivity. In previous studies on benzocyclobutene [34,45], dihalocyclopropanes [34,46], cyclobutane with diester attachments [11,44], and cyclobutane with diphenyl attachments [21], higher reactivity has always been observed when the pulling attachment stereochemistry is in the *cis* configuration. The higher reactivity of the *cis* attachment can be attributed to a more efficient coupling of force to the reaction coordinate, i.e., a more extended $\Delta x^{\dagger}$. For example, the $\Delta x^{\dagger}$ for *cis-gem*-difluorocyclopropane is 0.15 Å longer than that for the *trans* analogue (1.53 Å *vs*. 1.38 Å) [34]. In the case of benzocyclobutene, despite the significantly lower force-free reactivity of the *cis* stereoisomer, it still shows a higher force-coupled reactivity, as quantified by SMFS [34]. The change in the preference of reactivity when force is applied suggests that the advantage in force coupling can override the difference in force-free reactivity.

The stereochemical effect on the reactivity of cyclobutane has been quantified with SMFS by Zhang, Weng, and Boulatov [21]. In their study, the authors made both *cis*- and *trans*-diphenyl substituted cyclobutane mechanophores through dimerization of cinnamate, and they found that the forces required to activate the *cis*- and *trans*-diphenyl cyclobutanes on the timescale of 100 ms are 1 and 2 nN, respectively (Figure 7a). The stereochemical effect was also investigated by Wang and co-workers [12] in their mechanochemical cycloreversion of cyclobutane-fused tetrahydrofuran system. They synthesized *cis*- and *trans*-cyclobutane-fused tetrahydrofuran and polymers with identical initial molecular weight (89 kDa) and sonicated both polymers for 30 min, and they found that the ring opening percentages to be 38% and 29%, respectively (Figure 7b).

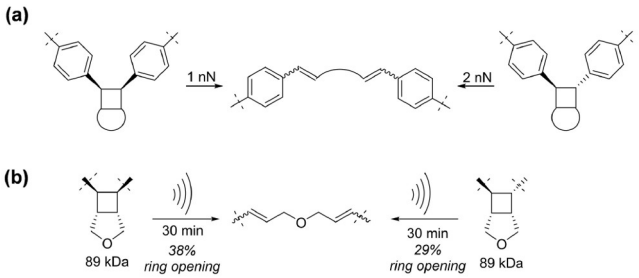

Figure 7 (a, b) Examples of the stereochemical effect in the mechanochemical cycloreversion of cyclobutane.

2.4 Regiochemical effect

The regiochemistry of pulling attachments is another structural factor that can be altered to control mechanochemical reactivity. The impact of pulling attachment regiochemistry has been demonstrated in spiropyran [47–49], naphthopyran [50] and Diels-Alder adducts [51]. Similar to the attachment stereochemical effect, altering attachment regiochemistry would normally lead to a change in $\Delta x^{\dagger}$, but the regiochemical effect can be more dramatic. In several cases, altering attachment regiochemistry could turn on or off the mechanochemical activation [50,51]. For example, Robb *et al*. [50] demonstrated that the mechanochemical activation of naphthopyran occurred only in one of the three regioisomers. The regiochemical effect in turning on/off mechanochemical reactivity has been observed in 1,2- (on) and 1,3-substituted (off) cyclobutane [52] as well as 1,2- (off), 1,3- (off) and 1,4-subsituted (off) cubane [20].

Recently, Xia and co-workers [53] reported the regiochemical effect of *cis*-diphenyl cyclobutane (Figure 8a). They synthesized diphenyl cyclobutane with attachments at the *ortho*-, *meta*-, and *para*-positions and compared the relative reactivity with *cis-gem*-dichlorocyclopropane (*cis*-*g*DCC), a mechanophore with previously quantified reactivity (1.3 nN is required to activate *cis*-*g*DCC on the timescale of 100 ms) [54]. This comparison was done by synthesizing copolymers of each regioisomer with *cis*-gDCC and sonicating the copolymer for 60 min. They found that the ring-opening ratios between the diphenyl cyclobutane and *cis*-*g*DCC for *ortho*- *meta*-, and *para*-regioisomers were 0.66, 0.79, and 1.67, respectively. The highest mechanochemical reactivity for the *para*-diphenyl cyclobutane was attributed to the most efficient coupling of force to the reaction coordinate, as quantified by the lowest stiffness of the ground state k_{eff}:k_{eff} for *ortho*- *meta*-, and *para*-regioisomers were calculated to be 23.2, 19.8, and 9.2 nN/Å, respectively. This approach of using the stiffness of the ground state to account for the mechanochemical coupling, which has recently been published by Moore and co-workers [55], is consistent with the treatment using the activation length $\Delta x^{\dagger}$.

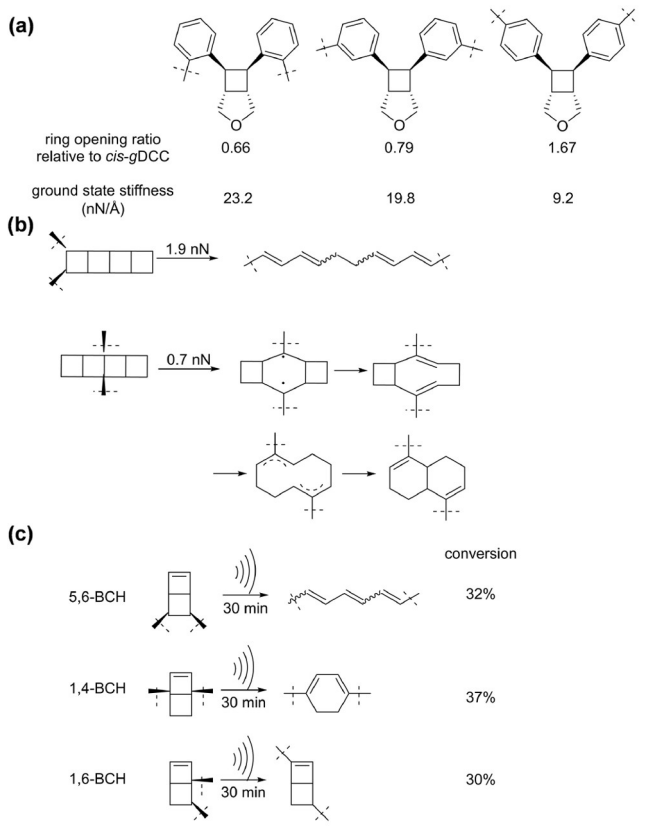

Figure 8 (a–c) Examples of the regiochemical effect in the mechanochemical cycloreversion of cyclobutane.

Xia and co-workers [43] also reported another interesting example of the regiochemical effect in their work on the mechanochemical cycloreversion of [4]-ladderane (Figure 8b). When pulled from the central rung, the molecule exhibited a significantly lower threshold force for mechanochemical activation on the timescale of 100 ms (0.7 nN) compared to when pulled from the end rung (1.9 nN). Unlike other regiochemical effects discussed above, the drastically different reactivity here was attributed to different intrinsic reactivity, i.e., different k_0, as reflected in the different bond lengths (1.62 Å *vs*. 1.58 Å) and the different stabilities of the diradical intermediates.

Another intriguing example of the stereochemical effect was reported by Liu and co-workers [56] in their study on a bicyclo[2.2.0]hexene (BCH) mechanophore. In their work, they found that the mechanochemical activation on 5,6-, 1,4-, and 1,6 positions of BCH resulted in retro-[2+2] cycloreversion, retro-4π ring-opening, and 1,3-allylic migration, respectively (Figure 8c). In addition, these pathways showed different reactivity: after sonicating each polymer with an initial molecular weight of ~60 kDa for 30 min, the mechanochemical conversions for 5,6-, 1,4-, and 1,6-BCHs were found to be 32%, 37%, and 30%.

3 Dynamics and stereoselectivity

The dynamics of the mechanochemical cycloreversion of cyclobutane have received great attention from the community. The dynamics also dictate the stereochemistry of the resulting alkenes. In this section, we discuss the dynamics of the mechanochemical cycloreversion and how it impacts the stereoselectivity of the alkene products.

An interesting observation in the mechanochemical cycloreversion of the BCO mechanophore was that the *EZ* alkene was the predominant product for both *cis*- and *trans*-BCO (Figure 9a, b), indicating that while the stereochemistry was largely retained during the cycloreversion of *trans*-BCO, the rotation of the C1–C4 bond or the C2–C3 bond in the diradical intermediate occurred preferentially during the cycloreversion of *cis*-BCO (Figure 9c), leading to the observed stereochemical distributions. To further probe the mechanism, the authors introduced steric hindrance at specific positions in the BCO structure by adding substituents such as nitrile and bromine groups. The addition of these groups hindered rotation in the diradical intermediate, which led to increased retention of the starting stereochemistry in the product, particularly with the bromine-substituted BCO, where the majority of the product showed retention of the original *cis* configuration. This study demonstrates that the stereochemical outcome of the mechanochemical reaction can be influenced by both the initial stereochemistry of the BCO and by steric effects that restrict rotation in the diradical intermediate, offering insight into the design of stress-responsive materials with controlled reactivity and product selectivity.

The stereoselectivity of cyclobutane was also studied by Wang and co-workers in their work on the mechanochemical cycloreversion of a cyclobutane-fused lactone (CBL) mechanophore (Figure 10). The fractions of the four stereoisomeric combinations—*EE*, *EZ*, *ZE*, and *ZZ*—were quantified as 43%, 21%, 33%, and 3%, respectively. The trend of $EZ+ZE > EE > ZZ$ aligns with the observations made by Kean *et al*. [11] as discussed above. However, the fraction of the *EE* configuration in this case is significantly higher (43% *vs*. 17%). Formation of the EE isomer requires stereochemical inversion at the C1–C4 bond and retention at the C2–C3 bond. A detailed analysis indicates that the C1–C4 bond is more prone to stereochemical inversion (64%), while the C2–C3 bond is more likely to retain its configuration (76%). This difference in retention *vs*. inversion tendencies, which was not present in the earlier BCO system, is likely due to structural asymmetry: C1–C4 is connected to an ester group, while C2–C3 is attached to a methylene group, suggesting that the functional groups on C4 and C3 also influence the rotation along the C1–C4 bond and C2–C3 bond. In other words, the ester group on C4 facilitates the rotation along the C1–C4 bond whereas the alkyl group on C3 dis-

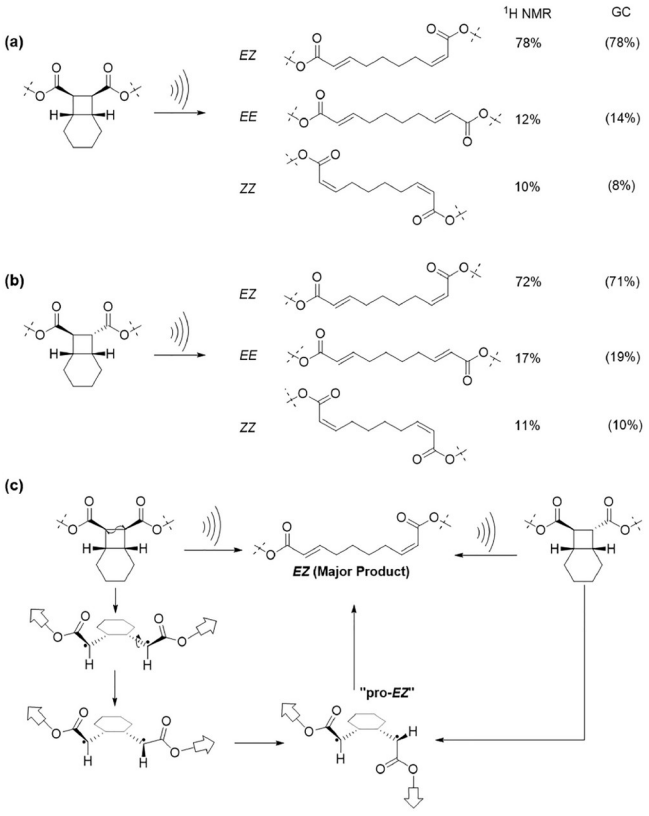

Figure 9 Stereoselectivity in the mechanochemical cycloreversion of the bicyclo[4.2.0]octane (BCO) mechanophore. (a, b) Product distribution for the mechanochemical activation of *cis*- and *trans*-BCO, respectively. (c) Mechanism for the mechanochemical cycloreversion of BCOs.

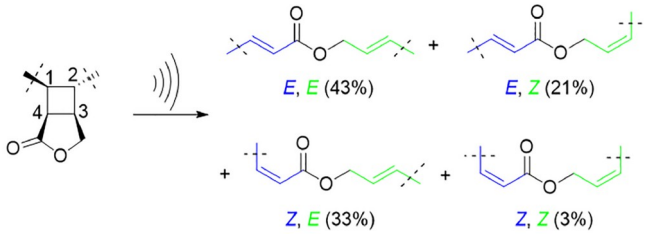

Figure 10 (Color online) Product distribution for the mechanochemical cycloreversion of cyclobutane-fused lactone (CBL).

favors the rotation along the C2–C3 bond, consistent with the limited bond rotation in the *trans*-BCO mechanophore.

While the stereochemical inversion was favored for *cis*-BCO (Figure 9), the stereochemistry was largely retained for the *cis*-cyclobutane-fused tetrahydrofuran (CBT) reported by Wang and co-workers (Figure 11) [12]. The different trends for BCO *vs*. CBT were attributed to the different attachments on them—ester groups are attached to BCO while alkyl groups are attached to CBT. The 1,4-diradical from the alkyl-substituted cyclobutane is expected to have a shorter lifetime and therefore is less likely to undergo rotation.

In 2020, Xia and co-workers [27] reported the dynamics of

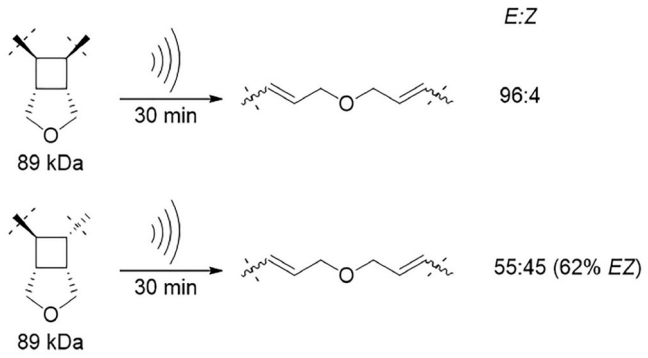

Figure 11 Product distribution for the mechanochemical cycloreversion of cyclobutane-fused tetrahydrofuran (CBT).

the mechanochemical cycloreversion of cyclobutane. The authors replaced the previously used ladderene with ladderane, which can be mechanically activated into a structure that is not completely conjugated, allowing for a detailed study of stereoselectivity. It was found that while the first cyclobutane formed *E*,*E* double bonds, the second cyclobutane formed a mixture of *E*,*E* and *E*,*Z* double bonds (Figure 12). *Ab initio* steered molecular dynamics (AISMD) showed that the cycloreversion of the second cyclobutane is accelerated by the cycloreversion of the first one. In other words, the remaining kinetic energy from the cycloreversion of the first cyclobutane has an effect on the cycloreversion of the second cyclobutane. Notably, the branching ratio from the mechanochemical cycloreversion of the second cyclobutane (*E*,*E*:*E*,*Z*=4:1) differs from what would be expected from the transition state theory (*E*,*E*:*E*,*Z*=1:4), representing a non-statistical dynamic effect (NDE) in mechanochemistry. It is worth mentioning that NDE was also observed by Wang and Craig *et al*. [57] in the branching ratio of the stereochemistry of *gem*-difluorocyclopropane from a mechanically trapped and then released diradical transition state.

Moore and co-workers [28] also studied the role of applied force in inducing and controlling NDEs for the mechanochemical cycloreversion of cyclobutane. They synthesized *anti* (A), *down* (D), and *up* (U) isomers for alkyl-substituted cyclobutanes (Figure 13a) as well as A and D isomers for ester-substituted cyclobutanes (Figure 13b) and incorporated each isomer at the center of a polymer. They then sonicated these polymers and characterized the stereochemistry of the alkene products. All the isomers of cyclobutane (including A, D, and U isomers for the alkyl-substituted cyclobutane and the A and D isomers for the ester-substituted cyclobutane) showed high stereoselectivity, although reduced stereoselectivity was observed for the ester-substituted ones (Figure 13b), likely due to torsional rotations. The authors attributed the high stereoselectivity to flyby reaction trajectories that occur when the reaction intermediates, 1,4-diradical in this case, do not have enough time to equilibrate thermally and instead proceed rapidly through the reaction

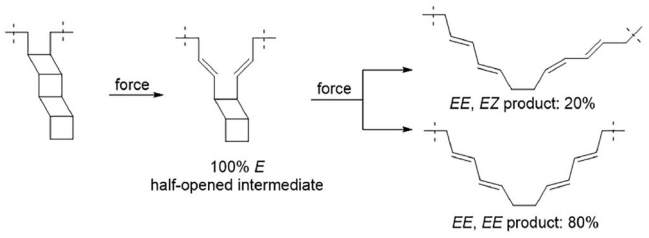

Figure 12 Product distribution for the mechanochemical cycloreversion of ladderane.

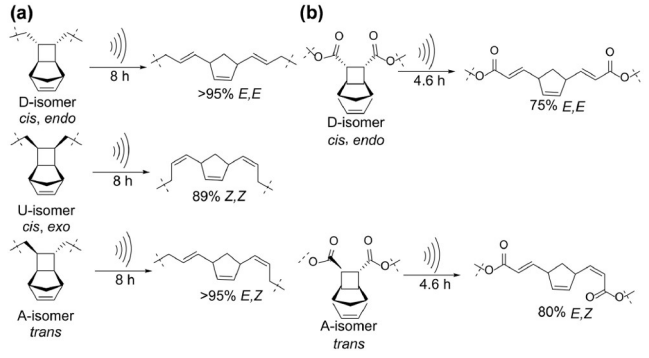

Figure 13 Product distribution for the mechanochemical cycloreversion of alkyl- (a) and ester-substituted (b) cyclobutane with various stereochemistry.

pathway due to the influence of external force. Notably, the single-mechanophore system here showed higher stereoselectivity than the multi-mechanophore systems by Craig and co-workers [11] and Wang and co-workers [12,58]. The reduced stereoselectivity displayed in the multi-mechanophore polymers is likely due to the different magnitude of force experienced by mechanophores distributed along different locations of the polymers.

4 Advancements in material design

When incorporating a mechanophore into a polymer network, based on the type of mechanophore (scissile *vs*. nonscissile) and its location in the network (on polymer strands *vs*. at crosslink junctions), the resulting topological outcomes upon mechanochemical activation include four scenarios (Figure 14). For example, the activation of a scissile mechanophore would lead to the breakage of a strand (Figure 14a) or a reduction in the crosslink density (Figure 14c) while the activation of a nonscissile mechanophore does not disrupt the integrity of the network. The intriguing mechanochemical reactivity of cyclobutane, combined with its thermal and chemical stability, makes it an ideal mechanophore to test the impact of mechanochemical activation on material properties. Recently, Craig's group [29–31] incorporated both scissile and nonscissile cyclobutane-based mechanophores into the strands and crosslink junctions of

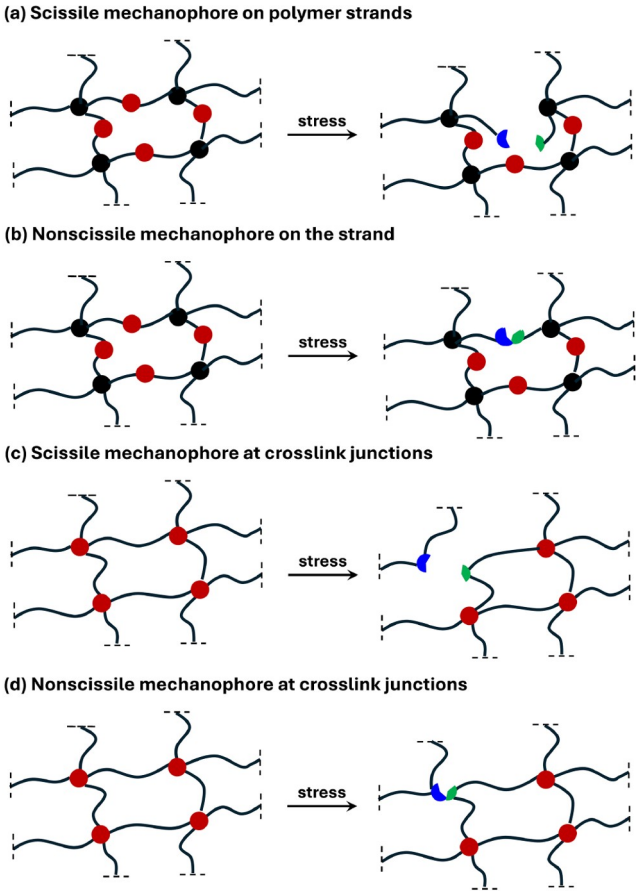

Figure 14 (Color online) (a–d) Four scenarios of topological outcomes from mechanophore activation in a network based on the type and location of the mechanophore.

polymer networks and investigated the impact on material properties.

In 2021, Craig and co-workers [29] synthesized three gels with various scissile links on their strands, including a *cis*-diphenyl cyclobutane link, a *cis*-dialkyl cyclobutane link, and a link without cyclobutane (Figure 15). This design falls into the category shown in Figure 14a. All networks exhibited similar linear elasticity (G' = 23–24 kPa, 0.1–100 Hz) and equilibrium swelling ratios in tetrahydrofuran (Q = 10–11), but they showed a wide range in tearing energies: 3.4 J m^{-2} for network with diphenyl cyclobutane link, 10.6 J m^{-2} for network with dialkyl cyclobutane link, and 27.1 J m^{-2} for network with a link that does not contain cyclobutane. The difference in fracture energy is attributed to variations in the mechanochemical reactivity of these links. The authors noted that the correlation between the fracture energy and the mechanical strength of bonds highlights the limitations of the Lake-Thomas theory, which relates the fracture energy of a network to the bond dissociation energy of the links in the polymer strands [59]. According to the Lake-Thomas theory, because the breakage of the diphenyl cyclobutane is exothermic, no energy is required. Thus, the

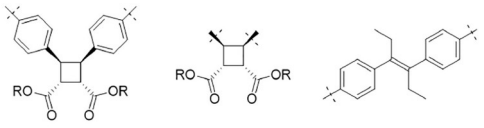

storage modulus G' (kPa)	23.0 ± 1.8	23.2 ± 0.8	24.4 ± 2.0
equilibrium mass swelling ratio Q	10.9 ± 1.1	11.3 ± 0.5	10.5 ± 0.9
tearing energy (J m^{-2})	3.4 ± 1.5	10.6 ± 1.7	27.1 ± 1.6

Figure 15 Mechanical properties of gels with different types of scissile links on their strands.

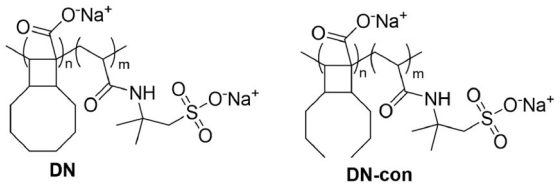

	E (kPa)	ε_b	σ_b (MPa)	W_b (MJ m^{-3})	ε_p	T (J m^{-2})
DN1	288 ± 4	10	0.92	6.4	2.3	2840 ± 103
DN1-con	290 ± 8	4.9	0.61	2.3	1.7	1419 ± 52
DN2	243 ± 5	7	0.64	2.6	1.3	554 ± 40
DN2-con	249 ± 13	4.7	0.54	1.6	0.8	276 ± 10
PAAm	57 ± 6	5	0.18	0.4	-	~100

Figure 16 Mechanical properties of double network hydrogels with nonscissile (DN) and scissile (DN-con) on the strands of their first networks. DN1 and DN2 differ in the crosslink density of the first network. E refers to Young's modulus; ε_b refers to nominal strain; σ_b refers to nominal stress; W_b refers to input energy density; ε_p refers to crack propagation strain; T refers to tearing energy. The tearing energy of PAAm gel is listed as reported by Ref. [53]. Dash indicates value not measured.

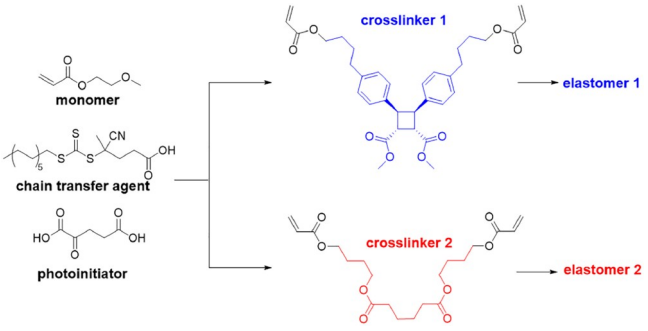

Figure 17 (Color online) Synthesis of elastomers with and without scissile cyclobutane mechanophore at their crosslink junctions.

fracture energy would be zero. Therefore, it is the mechanochemical kinetics (instead of the thermodynamic stability) of the breaking link that dictates the fracture energy.

In another 2021 study by Craig and co-workers [30], they studied the impact of the mechanically released stored length of nonscissile mechanophores on the fracture energy of hydrogel. A nonscissile cyclobutane-based mechanophore was installed on the polymer strands of the first network of a double network, and another double-network hydrogel with a scissile cyclobutane-based mechanophore was used as the control (Figure 16). The double-network hydrogel with the cyclobutane mechanophores also showed improved mechanical properties compared with a previously reported single-network polyacrylamide hydrogel [60]. Compared with control samples with scissile cyclobutane-based mechanophore, the incorporation of nonscissile cyclobutane-based mechanophore led to resistance of tearing in the double network materials, leading to a 40% increase in critical stretch for crack propagation and roughly double the tearing energy. This work highlights the benefit of placing nonscissile mechanophores on the strands of polymer networks (Figure 14b).

In 2023, Craig and co-workers [31] reported that incorporating scissile cyclobutane-based mechanophores at the crosslink junctions of a network can enhance the toughness of the network. They synthesized elastomers with and without a cyclobutane mechanophore at their crosslink junctions (elastomers **1** and **2** in Figure 17) and conducted tensile testing for both elastomers, finding that elastomer **1** showed higher toughness than that of elastomer **2** by up to 9 times. This network design corresponds to the scenario shown in Figure 14c. In addition, the authors also synthesized an elastomer with a nonscissile cyclobutane-based mechanophore (Figure 14d) and found that its toughness was comparable to that of elastomer **2**. The increased toughness in elastomer **1** was attributed to the selective breakage of the cyclobutane that converts cyclic defects into elastically active strands. Taken together, both the type (scissile *vs*. nonscissile) and the location (on the strands *vs*. at the crosslink junctions) of mechanophores are important in designing mechanically active polymer networks.

5 Conclusions and perspective

The cyclobutane mechanophore has brought insights into the understanding of chemomechanical processes and the design of next-generation polymeric materials. We expect that these insights discussed in this Mini Review will provide guidance to the continued development and implementation of cyclobutane mechanochemistry and polymer mechanochemistry in general. In addition, we also provide the following perspectives.

The reactivity, mechanism, and dynamics have been extensively studied in the context of SMFS and ultrasonication. We expect that new techniques for structural characterization and computational modeling will be applied to further understand the mechanochemical coupling processes. Recently, several studies have shown that the cyclobutane mechanophore can also be efficiently activated by ball milling [12,61,62], which can be done under solvent-free conditions and adds practicality value to the mechanochemical processes. Since the magnitude of the force and its distribution along the polymer backbone during ball milling of polymers

are expected to be different from those in SMFS and ultrasonication, the reactivity, mechanism, and stereoselectivity discussed above could be different and should be re-examined.

The incorporation of cyclobutane-based mechanophores, with both scissile and nonscissile types, on polymer strands and at crosslink junctions of polymer networks shows that the molecular reactivity of mechanophores and the topological design of the network are both instrumental in designing mechanophore-containing polymer networks. We expect that the knowledge of cyclobutane will be applied to other mechanophores to examine the current understanding with respect to how the type and the location of a mechanophore can impact material properties. In addition, the innovation in polymer network design will further enrich the toolbox for designing next-generation mechanically responsive polymeric materials [63,64].

Acknowledgements This work was supported by the National Science Foundation (CHE-2204079). R.O. acknowledges a Research Trainee Fellowship supported by the National Science Foundation (DGE-2152210). J. W. acknowledges the Alfred P. Sloan Foundation for a Sloan Research Fellowship (FG-2023-20341) and the Camille and Henry Dreyfus Foundation for a Camille Dreyfus Teacher-Scholar Award (TC-24-087).

Funding note Open Access funding enabled and organized by OhioLINK.

Conflict of interest The authors declare no conflict of interest.

1 Brown CL, Craig SL. *Chem Sci*, 2015, 6: 2158–2165
2 Potisek SL, Davis DA, Sottos NR, White SR, Moore JS. *J Am Chem Soc*, 2007, 129: 13808–13809
3 Ramirez ALB, Kean ZS, Orlicki JA, Champhekar M, Elsakr SM, Krause WE, Craig SL. *Nat Chem*, 2013, 5: 757–761
4 Davis DA, Hamilton A, Yang J, Cremar LD, Van Gough D, Potisek SL, Ong MT, Braun PV, Martínez TJ, White SR, Moore JS, Sottos NR. *Nature*, 2009, 459: 68–72
5 Huo S, Zhao P, Shi Z, Zou M, Yang X, Warszawik E, Loznik M, Göstl R, Herrmann A. *Nat Chem*, 2021, 13: 131–139
6 Yao Y, McFadden ME, Luo SM, Barber RW, Kang E, Bar-Zion A, Smith CAB, Jin Z, Legendre M, Ling B, Malounda D, Torres A, Hamza T, Edwards CER, Shapiro MG, Robb MJ. *Proc Natl Acad Sci USA*, 2023, 120: e2309822120
7 Kean ZS, Craig SL. *Polymer*, 2012, 53: 1035–1048
8 Seubold FH Jr.. *J Chem Phys*, 1953, 21: 1616–1617
9 Genaux CT, Kern F, Walters WD. *J Am Chem Soc*, 1953, 75: 6196–6199
10 Chen Z, Mercer JAM, Zhu X, Romaniuk JAH, Pfattner R, Cegelski L, Martinez TJ, Burns NZ, Xia Y. *Science*, 2017, 357: 475–479
11 Kean ZS, Niu Z, Hewage GB, Rheingold AL, Craig SL. *J Am Chem Soc*, 2013, 135: 13598–13604
12 Hsu TG, Liu S, Guan X, Yoon S, Zhou J, Chen WY, Gaire S, Seylar J, Chen H, Wang Z, Rivera J, Wu L, Ziegler CJ, McKenzie R, Wang J. *Nat Commun*, 2023, 14: 225
13 Poplata S, Tröster A, Zou YQ, Bach T. *Chem Rev*, 2016, 116: 9748–9815
14 Bowser BH, Ho CH, Craig SL. *Macromolecules*, 2019, 52: 9032–9038
15 Kryger MJ, Ong MT, Odom SA, Sottos NR, White SR, Martinez TJ, Moore JS. *J Am Chem Soc*, 2010, 132: 4558–4559
16 Kean ZS, Black Ramirez AL, Yan Y, Craig SL. *J Am Chem Soc*, 2012, 134: 12939–12942
17 Wang J, Kouznetsova TB, Boulatov R, Craig SL. *Nat Commun*, 2016, 7: 13433
18 Zhou J, Hsu T, Wang J. *Angew Chem Int Ed*, 2023, 62: e202300768
19 Aydonat S, Hergesell AH, Seitzinger CL, Lennarz R, Chang G, Sievers C, Meisner J, Vollmer I, Göstl R. *Polym J*, 2024, 56: 249–268
20 Wang L, Zheng X, Kouznetsova TB, Yen T, Ouchi T, Brown CL, Craig SL. *J Am Chem Soc*, 2022, 144: 22865–22869
21 Zhang H, Li X, Lin Y, Gao F, Tang Z, Su P, Zhang W, Xu Y, Weng W, Boulatov R. *Nat Commun*, 2017, 8: 1147
22 Li M, Zhang H, Gao F, Tang Z, Zeng D, Pan Y, Su P, Ruan Y, Xu Y, Weng W. *Polym Chem*, 2019, 10: 905–910
23 Gunckel R, Koo B, Xu Y, Pauley B, Hall A, Chattopadhyay A, Dai LL. *ACS Appl Polym Mater*, 2020, 2: 3916–3928
24 Kean ZS, Gossweiler GR, Kouznetsova TB, Hewage GB, Craig SL. *Chem Commun*, 2015, 51: 9157–9160
25 Overholts AC, Robb MJ. *ACS Macro Lett*, 2022, 11: 733–738
26 He X, Tian Y, O'Neill RT, Xu Y, Lin Y, Weng W, Boulatov R. *J Am Chem Soc*, 2023, 145: 23214–23226
27 Chen Z, Zhu X, Yang J, Mercer JAM, Burns NZ, Martinez TJ, Xia Y. *Nat Chem*, 2020, 12: 302–309
28 Liu Y, Holm S, Meisner J, Jia Y, Wu Q, Woods TJ, Martinez TJ, Moore JS. *Science*, 2021, 373: 208–212
29 Wang S, Beech HK, Bowser BH, Kouznetsova TB, Olsen BD, Rubinstein M, Craig SL. *J Am Chem Soc*, 2021, 143: 3714–3718
30 Wang Z, Zheng X, Ouchi T, Kouznetsova TB, Beech HK, Av-Ron S, Matsuda T, Bowser BH, Wang S, Johnson JA, Kalow JA, Olsen BD, Gong JP, Rubinstein M, Craig SL. *Science*, 2021, 374: 193–196
31 Wang S, Hu Y, Kouznetsova TB, Sapir L, Chen D, Herzog-Arbeitman A, Johnson JA, Rubinstein M, Craig SL. *Science*, 2023, 380: 1248–1252
32 Robb MJ, Moore JS. *J Am Chem Soc*, 2015, 137: 10946–10949
33 Lin Y, Chang CC, Craig SL. *Org Chem Front*, 2019, 6: 1052–1057
34 Wang J, Kouznetsova TB, Niu Z, Ong MT, Klukovich HM, Rheingold AL, Martinez TJ, Craig SL. *Nat Chem*, 2015, 7: 323–327
35 Dudko OK, Hummer G, Szabo A. *Phys Rev Lett*, 2006, 96: 108101
36 Boulatov R. *Pure Appl Chem*, 2010, 83: 25–41
37 Konda SSM, Brantley JN, Bielawski CW, Makarov DE. *J Chem Phys*, 2011, 135: 164103
38 May PA, Moore JS. *Chem Soc Rev*, 2013, 42: 7497–7506
39 Wu D, Lenhardt JM, Black AL, Akhremitchev BB, Craig SL. *J Am Chem Soc*, 2010, 132: 15936–15938
40 Wang J, Kouznetsova TB, Craig SL. *J Am Chem Soc*, 2016, 138: 10410–10412
41 Brown CL, Bowser BH, Meisner J, Kouznetsova TB, Seritan S, Martinez TJ, Craig SL. *J Am Chem Soc*, 2021, 143: 3846–3855
42 Horst M, Yang J, Meisner J, Kouznetsova TB, Martínez TJ, Craig SL, Xia Y. *J Am Chem Soc*, 2021, 143: 12328–12334
43 Horst M, Meisner J, Yang J, Kouznetsova TB, Craig SL, Martínez TJ, Xia Y. *J Am Chem Soc*, 2024, 146: 884–891
44 Kryger MJ, Munaretto AM, Moore JS. *J Am Chem Soc*, 2011, 133: 18992–18998
45 Hickenboth CR, Moore JS, White SR, Sottos NR, Baudry J, Wilson SR. *Nature*, 2007, 446: 423–427
46 Lenhardt JM, Black AL, Craig SL. *J Am Chem Soc*, 2009, 131: 10818–10819
47 Gossweiler GR, Kouznetsova TB, Craig SL. *J Am Chem Soc*, 2015, 137: 6148–6151
48 Kim TA, Robb MJ, Moore JS, White SR, Sottos NR. *Macromolecules*, 2018, 51: 9177–9183
49 Lin Y, Barbee MH, Chang CC, Craig SL. *J Am Chem Soc*, 2018, 140:

15969–15975
50 Robb MJ, Kim TA, Halmes AJ, White SR, Sottos NR, Moore JS. *J Am Chem Soc*, 2016, 138: 12328–12331
51 Stevenson R, De Bo G. *J Am Chem Soc*, 2017, 139: 16768–16771
52 Groote R, Szyja BM, Leibfarth FA, Hawker CJ, Doltsinis NL, Sijbesma RP. *Macromolecules*, 2014, 47: 1187–1192
53 Flear EJ, Horst M, Yang J, Xia Y. *Angew Chem Int Ed*, 2024, 63: e202406103
54 Klukovich HM, Kouznetsova TB, Kean ZS, Lenhardt JM, Craig SL. *Nat Chem*, 2013, 5: 110–114
55 Sun Y, Kevlishvili I, Kouznetsova TB, Burke ZP, Craig SL, Kulik HJ, Moore JS. *Chem*, 2024, 10: 3055–3066
56 Ding S, Wang W, Germann A, Wei Y, Du T, Meisner J, Zhu R, Liu Y. *J Am Chem Soc*, 2024, 146: 6104–6113
57 Wang J, Ong MT, Kouznetsova TB, Lenhardt JM, Martínez TJ, Craig SL. *J Org Chem*, 2015, 80: 11773–11778
58 Hsu TG, Zhou J, Su HW, Schrage BR, Ziegler CJ, Wang J. *J Am Chem Soc*, 2020, 142: 2100–2104
59 Lake GJ, Thomas AG. *Proc R Soc Lond A*, 1967, 300: 108–119
60 Sun JY, Zhao X, Illeperuma WRK, Chaudhuri O, Oh KH, Mooney DJ, Vlassak JJ, Suo Z. *Nature*, 2012, 489: 133–136
61 Liu P, Jimaja S, Immel S, Thomas C, Mayer M, Weder C, Bruns N. *Nat Chem*, 2024, 16: 1184–1192
62 Zhang X, Zhao Y, Chen M, Ji M, Sha Y, Nozaki K, Tang S. *J Am Chem Soc*, 2024, 146: 24024–24032
63 Gu Y, Zhao J, Johnson JA. *Angew Chem Int Ed*, 2020, 59: 5022–5049
64 Lloyd EM, Vakil JR, Yao Y, Sottos NR, Craig SL. *J Am Chem Soc*, 2023, 145: 751–768